OPEN ACCESS

University of BRISTOL

Peer reviewed version

University of Bristol - Explore Bristol Research

General rights

11.2 Tb/s Classical Channel Coexistence with DV-QKD over a 7-Core Multicore Fiber

E. Hugues-Salas, O. Alia, R. Wang, K. Rajkumar, G. T. Kanellos, R. Nejabati and D. Simeonidou

Abstract—**The feasibility of transmitting discrete-variable quantum key distribution channels with carrier-grade classical optical channels over multicore fibers is experimentally explored in terms of achievable quantum bit error rates, secret key rates as well as classical signal bit error rates. A coexistence transmission record of 11.2 Tb/s is achieved for the classical channels simultaneously with a DV-QKD channel over a 1 km-long 7-core multicore fiber. Coexistence over the same multicore fiber core is identified as a dominant factor for the performance of the quantum channel requiring optical bandpass filtering of 17nm for the quantum channel to avoid the effect of Raman noise. Also, counter-propagation of classical channels and quantum channels probe more tolerance to noise proliferation than co-propagation. In addition, the performance of the quantum channel is maintained when more than three cores are used for the classical channels. Furthermore, by adding a second DV-QKD channel in the multicore fiber, the simultaneous transmission of classical channels as well as the generation of quantum-secured keys of two QKD channels is achieved with an operational range of 10dB of launched power into the MCF.**

Index Terms—**Quantum key distribution, bandwidth variable transceivers, multicore fiber, spatial division multiplexing, quantum and classical channel coexistence.**

I. INTRODUCTION

With current bandwidth demands exceeding the available spectrum capacity of single-mode optical fiber (SMF), multicore fibers (MCF) have been introduced as specialty fibers to address future bandwidth needs by exploiting the space division multiplexing (SDM) dimension [1]. Numerous MCF technologies and fiber profiles have been brought into perspective aiming to improve MCF characteristics such as the number of cores, crosstalk (XT) and coupling into the fiber. As a consequence of this research on MCFs over the last decade [2]-[4], initial MCF-based SDM deployments and field trials are being undertaken in different parts of the world, such as the testbeds in Japan and Italy [5]-[6]. In addition, since manufacturing costs of these specialized fibers and their cost of deployment in long reach communications is prohibitive and their main benefit is the reduction in physical space requirements, MCF primary field of application is considered to be the intra-data center (DC) links to decrease the density of current optical fiber bundles interconnecting the thousands of processing nodes [7].

However, in future datacenters, 94% of the total workloads and compute instances will be processed in the cloud as opposed to only 6% for the traditional datacenters [8]. In these emerging cloud datacenters, migration of workloads and compute instances is undertaken across servers, inside and between datacenters, for optimum datacenter workload balance and for maximum support to end-user applications. In this migration, cloud virtualization is the key factor, and dynamic deployment of workloads is enabled by moving virtual machine (VM) images between physical machines through the datacenter. This migration of virtual resources is vulnerable to attacks whenever VMs are in transit and in between secured perimeters and attackers can exploit the network vulnerability to gain unauthorized access to the VMs [9].

To provide security in these cloud datacenters, different protocols are used to protect the data whenever communication is required between servers and applications. A typical protocol widely used is the transport layer security (TLS) protocol to protect and authenticate communications across the Internet. TLS relies in part on asymmetric cryptography algorithms, such as Rivest–Shamir–Adleman (RSA) and Elliptic Curve Diffie-Hellman (ECDH), which are vulnerable to quantum computing attacks [10]. Therefore, to overcome this security weakness, improvements on this TLS and other protocols are required to prevent eavesdropping and tampering.

One effective method that will ensure the security within cloud data centers and that can be integrated with encryption protocols is quantum key distribution (QKD). Since QKD enables the distribution of symmetric keys, the integration of TLS with QKD has been suggested in several communications [11]-[13] and standards [14]. QKD has been identified as a future-proof data encryption technique that exploits the uncertainty principle of quantum mechanics to enable the recognition of an eavesdropper, Eve, tampering over an optical channel [15]. In QKD, whenever the distribution of symmetric keys is undertaken by transmitting single photons from a sender, Alice, to a receiver, Bob, and eavesdropping occurs over the quantum channel, Eve's measurements will generate significant error rates in the key data allowing Alice and Bob to be able to verify the secrecy of the key and detect the intrusion. Eve will also be prevented to learn the key, since any attempt to gain information about the photons will irreversibly change

E. Hugues-Salas, O. Alia, R. Wang, K. Rajkumar, G. T. Kanellos, R. Nejabati and D. Simeonidou are with High Performance Network Group, School of Computer Science, Electrical & Electronic Engineering and Engineering Maths (SCEEM), University of Bristol, UK (e-mail: e.huguessalas@bristol.ac.uk).
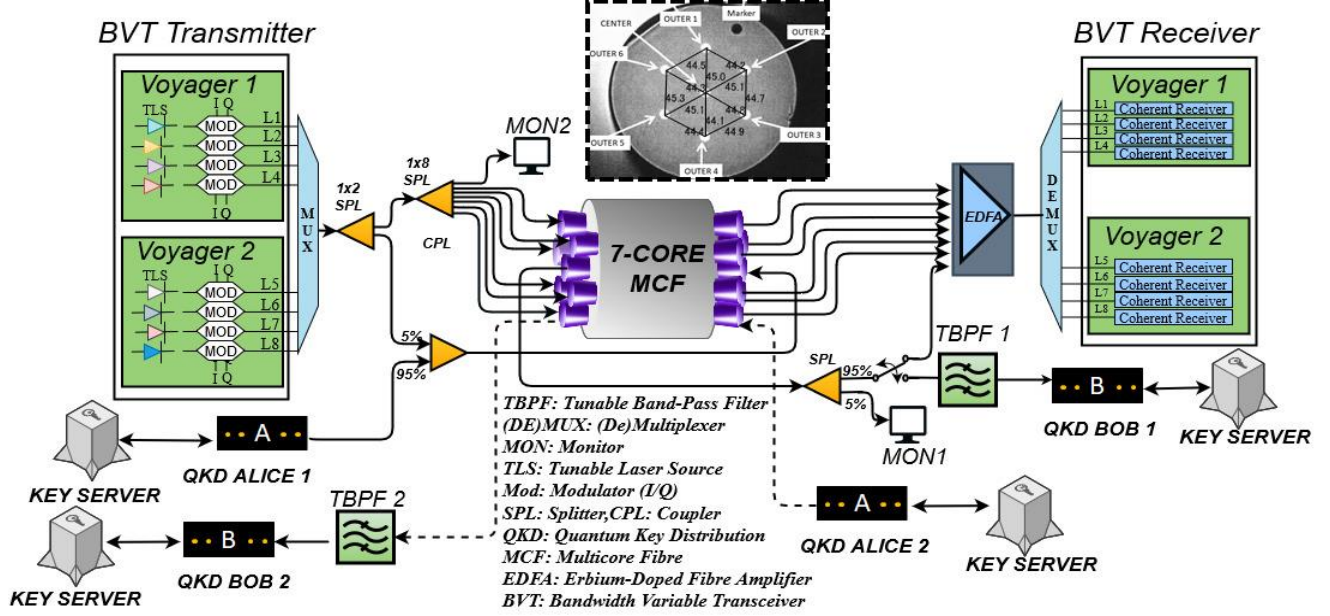
Fig. 1. Experimental Testbed for the Coexistence of 11.2Tb/s classical channels and QKD channels over a 7-core multicore fiber.
Inset: Cross-sectional Diagram MCF

them. Based on this secure QKD operation, we recently proposed and demonstrated the integration of QKD and a 5G orchestration platform in a quantum-secure exchange of information between distributed edge compute nodes [16]. In addition, based on this information theoretical secure QKD method, proof of concept testbeds have been demonstrated in Vienna, Cambridge, Tokyo, Battelle, Florence, China (Beijing-Shanghai), Madrid and recently Bristol [17]-[24] and system technologies have become commercial [25]-[26].

Nevertheless, since current commercially deployed discrete-variable QKD (DV-QKD) schemes rely on the exchange of single or few photons to transfer the quantum information, serious restrictions on the acceptable noise levels are imposed and overall optical insertion losses limit the operation of the DV-QKD link, rendering the deployment of quantum with classical optical communication channels very difficult. Therefore, a viable co-existing scheme is needed to guarantee large scale deployment of DV-QKD technologies in parallel to classical optical telecommunications.

Based on this coexistence requirement and the inherent advantages of MCFs, in recent publications [27][28], we reported the preliminary results to optimize the transmission capacity of the classical optical channels in the peripheral cores of an MCF while sustaining the viability of a single quantum channel in the central core. In this communication we generalize our approach and evaluate the system architecture with an additional QKD channel for increased coexistence levels of two quantum channels and classical channels over the same 7-Core MCF. We also present additional characterization of the MCF for bidirectional coexistence.

Results show that a maximum launch power of +5dBm is achieved with QBER of 2.5%, SKR of 1200 b/s and BER of 1.4 $\times 10^{-4}$ when the coexistence of classical and quantum channels is undertaken without including classical channels in the same core as the quantum channel. Moreover, with a maximum

launch power of -9.5 dBm of the classical channels coexisting with the quantum channel over the same core, an aggregate 11.2 Tb/s of classical channels is achieved for a BER of 6.68×10^{-4}, a QBER of 6.3% and a SKR of 73 b/s. With regards to the wavelength spacing between the quantum and classical channels for high capacity, a minimum channel spacing of 8.5nm is reached between the quantum channel and the nearest classical channel from lower and higher wavelengths. Finally, when a second quantum channel is added to the MCF for coexistence, a minimum QBER of 2.6% is achieved in this second channel, meanwhile the original first quantum channel maintains a QBER of 1.8%.

II. Literature Review on Coexistence of Quantum and Classical Channels

Several co-existing schemes that allow quantum channels and classical channels in the same optical medium have been proposed mainly relying on the principles of wavelength division multiplexing (WDM). Specifically, the first coexistence experiment [29] employed wavelength multiplexing and proposed the use of O-Band for the QKD channel (QC) and the use of C-band for the conventional channels (CC). Other state-of-the-art developments have demonstrated co-propagation of QKD with one 100 Gbps dense wavelength-division multiplexing (DWDM) data channel in 200 km ultra-low loss fiber [30] while in [22] data transmission of 3.6 Tb/s was achieved at 21 dBm launch power with the quantum channel at 1310 nm. However, as launching powers induce more noise and spectral proximity is prohibitive, WDM coexistence of CC and QC in the same frequency band is a compromise between launching powers, bandwidths and targeted secret key rates (SKR) for the quantum channels.

Another approach for achieving efficient coexistence levels lies with the use of SDM. In this case, multicore fibers offer enhanced channel isolation between cores and can in principle

allow the unconditional coexistence of QC and CC. For instance, in [31] the coexistence of QC and CC was demonstrated over a 7-core MCF with 2x10 Gb/s CCs and 0 dBm of launching power. In [32] the co-existence of QCs and CCs is presented in which the CCs were emulated by a continuous-wave (CW) and launching powers of +12 dBm. In [33], 6x112 Gb/s PAM signals were used as CCs and single-photon detection was used to verify the feasibility of co-existence of QCs and CCs. In this direction, MCFs have also been exploited to optimize the SKR of the QC by initiating the concept of high-dimensional quantum cryptography, and in [34] a spatial-multiplexed key rate of 105.7 Mb/s was demonstrated, coexisting with 37x10 Gb/s classical channels. All these advances demonstrate the suitability of QKD over multicore fibers for intra- and potentially inter- data center deployments, in which short MCF links can be promoted to support intense traffic and quantum secure communications between compute nodes in data centers.
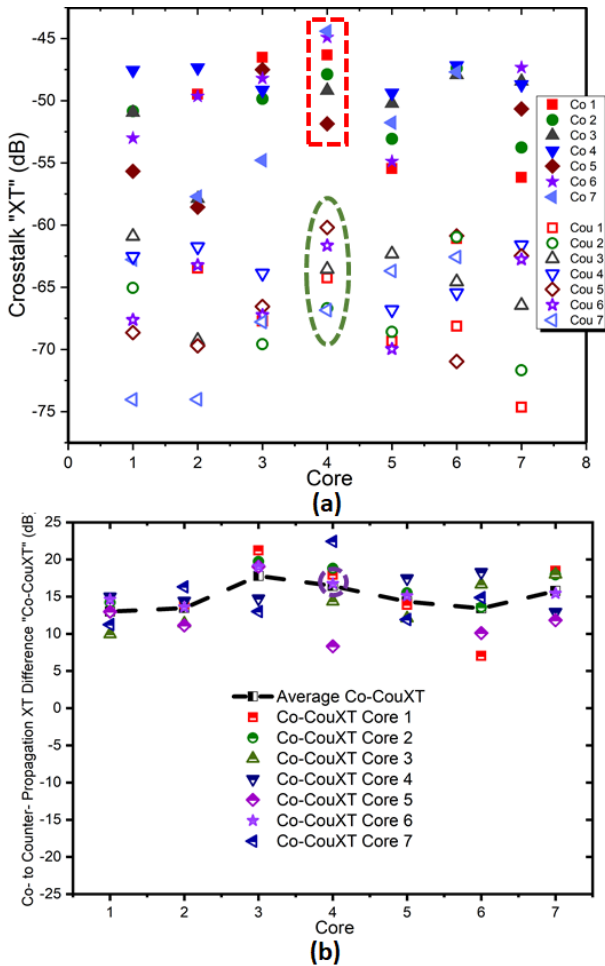

Fig. 2. a) Crosstalk characterization of the used MCF for co-propagation (Co) and counter-propagation (Cou) of optical signals. b) XT difference per core of the co-propagation to the counter-propagation of optical signals in the 7-core MCF used.

III. EXPERIMENTAL SYSTEM SETUP

Fig. 1 shows the experimental system setup used to demonstrate the coexistence of classical channels with QKD channels over a 1km-long 7-Core MCF (as inset figure, Fig. 1 also illustrates the cross-sectional diagram of the MCF used, fabricated by Mitsubishi). For the classical channels, two optical packet DWDM platforms are used with bandwidth-variable transponders (BVTs) [35],[36]. Each of these units include four BVT ports reconfigurable to coherent 100 Gb/s (PM-QPSK), 150 Gb/s (8-QAM) or 200Gb/s (16-QAM) and each port can be tuned to any of the 100 wavelengths in the C-band included in the ITU-T grid with 50GHz offset. Adaptable soft-decision forward error correction (SD-FEC) is also available in the transponders to enable maximum transmission capacity with minimum errors. In this experiment, all the ports where configured with 16-QAM modulation for a maximum of 200Gb/s per channel and the SD-FEC considered was 25%. For the quantum channels, IDQuantique DV-QKD systems are used (ID3100 Clavis^2 [37]). These QKD systems include an autocompensating interferometric set-up and quantum random number generators (QRNGs) to create secret keys. In addition, these Clavis 2 systems support fully automated sifting for the BB84 protocols and key distillation.

As shown in Fig. 1, the eight coherent output ports of the two BVTs are multiplexed using a wavelength selective switch (WSS) with ~5 dB of insertion loss for a total throughput of 1.6 Tb/s and its combined output feeds the input port of a 3 dB splitter which divides equally the multiplexed signal into two optical paths. One path is directed to a 10 dB-loss, 1x8 splitter, which further splits the multiplexed signal into eight different paths and six of them are directly connected to 6 cores of the MCF. The second path is coupled to the quantum channel via a coupler with 95/5% ratio and an insertion loss of ~13dB for the 5% port used to enable low power loss in the quantum channel. The second port of this 95/5% coupler is used to exchange the encoded photons of the discrete-variable DV-QKD Alice unit considering a power loss of <0.5 dB for the 95% port. The output of this 95/5% coupler is then injected into the center core of the 7-Core MCF which has an average core pitch of ~44.7 μm and a loss of 0.2 dB/km per core. In the MCF, these quantum and classical signals counter-propagate with the injected classical signals from the other cores, as shown in Fig. 1, for a combined data rate of 11.2 Tb/s for the classical channels.

After the coexistence within the MCF, the output of the center core feeds a 3.4 dB-loss, 2 nm 3 dB-bandwidth tunable-band pass filter (TBPF) tuned to the 1551.7 nm wavelength of the QKD unit. After the TBPF, the DV-QKD Bob unit undertakes the single-photon detection and processing of the encoded photon allowing the completion of the BB84 protocol of the DV-QKD systems. The output of the center core of the MCF is also directed to an optical amplification stage to set the classical signals to the suitable detectable power levels before demultiplexing via a 5 dB-loss WSS. This last WSS connects to the receiving ports of the BVT equipment for coherent reception and the outputs of the remaining outer cores of the MCFs are also connected to the amplification stage before demultiplexing and coherent detection of the classical channels. In this testbed, the total end-to-end (Alice to Bob) quantum

channel loss is 6.74 dB. A summary of main parameters of the testbed is shown in Table I.

TABLE I
PARAMETERS FOR MCF-BASED COEXISTENCE TESTBED

Parameters	Value
Classical Channels	
Number of Channels	8
Channel Wavelengths @minimum spacing	1561.83 nm, 1561.42 nm, 1561.01nm, 1560.61 nm, 1543.33 nm, 1542.94 nm, 1542.54 nm, 1542.14 nm.
Grid Spacing	50 GHz
Modulation format	16-QAM
Capacity per channel (CC)	200 Gb/s
Capacity per core (8 CCs)	1.6 Tb/s
Total capacity over MCF (8 CCs/7 Cores)	11.2 Tb/s
Pre-FEC level	25%
CC Detector Sensitivity [1]	-26 dBm
Quantum Channels	
DV-QKD Wavelength	1551.7 nm
QKD Protocol	BB84
Distance (maximum)	50 km@10 dB loss
Multicore Fiber	
Multicore Fiber Type	Step Index Core
Number of Cores	7
MCF Length	1 km
Propagation loss	0.2 dB/km @1550 nm
Inter-core crosstalk	-48 dB/km @1550 nm
Core Pitch	44.7 μm (average)
Tunable Optical Bandpass Filter	
Bandwidth @3dB	2 nm
Insertion loss	3.4 dB

[1] Corresponding to 16-QAM Modulation @200Gb/s and back-to-back.

In addition, as part of this testbed, a second QKD channel was integrated to demonstrate the coexistence of not only several classical channels but also two quantum channels over the MCF. Fig. 1 shows a second QKD Alice and Bob units interconnected via an outer core of the MCF and a TBPF. A key server is used per each QKD unit to undertake the quantum protocol and to retrieve the keys generated by the quantum
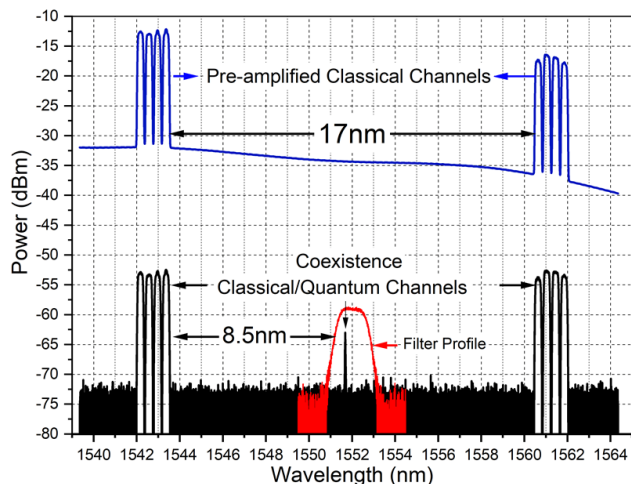
Fig. 3. Spectrum of the combined transmission over a single core of quantum and classical channels.

channels. These key servers use as classical channel a standard ethernet connection to undertake the post-processing required to transform the photons exchanged via QKD into secure keys.

IV. MCF CHARACTERIZATION

Fig. 2 shows the static XT characterization of the 1km-long 7-core MCF. In here, the measured XT is the difference of the injected optical power of a continuous wave (CW) on a selected core from the observed output power of another core. Co- and counter-propagation is measured by observing the output power at the input or output ports of the MCF. To characterize this type of crosstalk, the central core (core 4) was assigned with the QKD channel and the outer cores with the classical channels representing the worst-case scenario. This configuration allows an equal impact of the classical channels over the QKD channel enabling a suitable evaluation of the feasibility of QKD and classical signals simultaneously over a MCF [31],[33].

As observed in Fig. 2a, core 4 (central core) is the most affected with a range of XT levels from -51 dB to -44 dB for the case of co-propagation (dashed square, Fig. 2a) and for the case of counter-propagation, the XT levels of core 4 vary from -66 dBm to -60 dBm (dashed ellipse, Fig. 2a), being evident that the effect of XT due to counter-propagation is lower compared to the one due to co-propagation, as described in [32], [38].

Fig. 2b shows the measured co- to counter- propagation XT difference (Co-CouXT) per core of the MCF. As observed, in the selected core 4, an additional average tolerance of 16.5 dB to XT is measured whenever counter-propagation of optical signals is used (dashed circle, Fig. 2b). Therefore, for this experiment, counter-propagation of quantum to classical signals was selected, with the quantum channel in the central core (core 4) since XT isolation determined the performance of the entire system for coexistence.
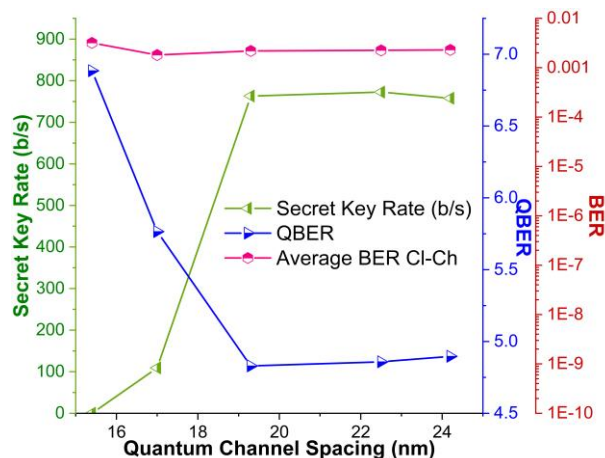
Fig. 4. SKR, QBER and BER vs channel spacing between the quantum and classical channels of the MCF central core.
(Total capacity for CCs is 11.2 Tb/s)

V. EXPERIMENTAL RESULTS

A. Quantum and Classical Channel Coexistence over a Single Core of the MCF

Fig. 3 shows the spectrum of the 8x200 Gb/s classical channels coexisting with the quantum channel over the central core of the MCF, obtained by using a tap coupler in the quantum channel (Fig. 1). As a reference, Fig. 3 illustrates the optical filter profile used to filter out the Raman noise generated by the classical channels in the quantum channel. Fig. 3 also shows the transmitted classical signals after passing through an adjacent core of the MCF before demultiplexing and coherent detection in the receiver (Fig. 1).
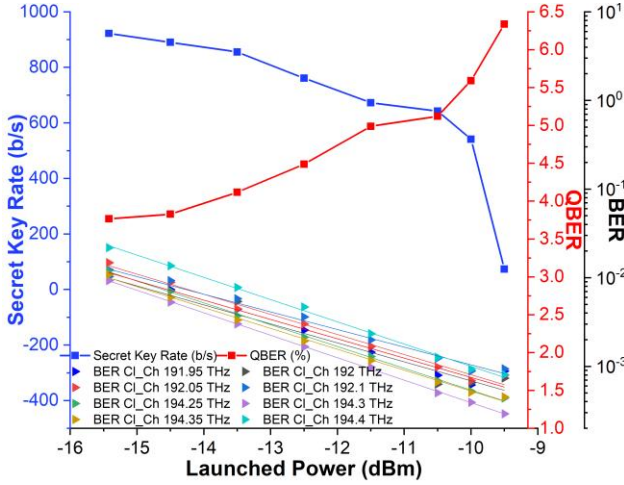

Fig. 5. SKR, QBER and BER versus launched optical power of the central core of the 7-core multicore fiber. (Total capacity of CCs is 11.2 Tb/s)

B. Channel Spacing for Coexistence over a Single Core

To further investigate the effect of the classical channels over the quantum channel over the same core, Fig. 4 illustrates the performance of the coexisting channels by decreasing the spectral spacing between them. A minimum spacing of 17nm between non-contiguous channels (Fig. 3) was observed with a measured QBER of 5.7% and a secret key rate of 100 b/s, for the quantum channel, and an average BER of 1.8×10^{-3} for the classical channels being considerably lower than the SD-FEC limit enabled by the BVT (Fig. 4). Beyond this minimum spacing, the QKD system stops generating keys.

The transmission over the other cores with 1.6 Tb/s per core was undertaken in parallel with the DV-QKD channel without the performance of these channels being affected, since the XT of the MCF enabled the coexistence with a total of 11.2 Tb/s. To enable this high capacity coexistence, counter-propagation of quantum and classical channels was used, as shown in Fig. 1, to allow additional XT tolerance shown in Fig. 2.

C. Performance Evaluation of the Coexistence of a DV-QKD Channel and 11.2 Tb/s Classical Channels over a 7-core Multicore Fiber

While transmitting 1.6 Tb/s through each outer core of the MCF and the central core, Fig. 5 shows the resulting curve of the SKR, QBER and BER vs launch power for the transmission

of eight 16-QAM-modulated optical channels and a DV-QKD channel over the central core of the MCF. For this Fig. 5, the power levels of individual channels were increased from the BVT interfaces to increase the launched power. As observed, the QBER increases and the SKR decreases when the launched optical power into the MCF is increased up to a maximum power of -9.5 dBm. Beyond this limit, the system stops generating keys due to excessive Raman noise leakage over the quantum channel. This launched power into the MCF was improved by removing the CCs from the central core to a launched power of +5 dBm, however, the coexistence capacity was reduced to 9.8 Tb/s. Table II shows a summary for the different launched powers and central core configurations.

TABLE II
LAUNCHING POWERS FOR DIFFERENT COEXISTENCE CAPACITIES

Central Core	Launch Power	Capacity	QBER	SKR	BER
QC only	+5dBm	9.8Tb/s	2.5%	1.2Kb/s	1.4×10^{-4}
QC/CCs	-9.5dBm	11.2Tb/s	6.3%	73b/s	6.68×10^{-4}

To explore the impact of the coexistence from adjacent cores of the MCF, Fig. 6. shows the performance of the quantum and classical channels after adding channels incrementally at different outer cores. To clearly notice this effect, the TBPF before the QKD Bob unit is not used. However, CCs are not used in the central core since the Raman noise generated will not be tolerable by the QC. Therefore, the total capacity in the MCF will be 9.6 Tb/s for the CCs.
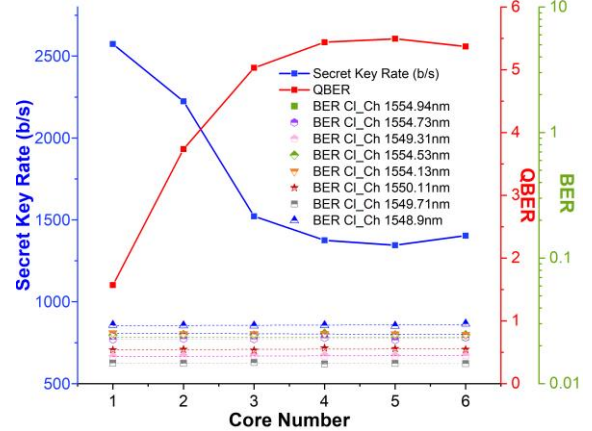

Fig. 6. SKR, QBER and BER vs combined number of cores with classical channels. Total capacity is 9.6 Tb/s (No added CCs in central core).

As observed in Fig. 6, for the first two added cores, the quantum channel QBER and SKR are kept within the limits of 3.5% and 2220 b/s, respectively. Beyond three added cores, the performance degrades to 5% (QBER) and 1520 b/s (SKR). However, the same performance is kept when adding classical signals for the total six additional cores.

To further investigate the coexistence over the MCF, a second DV-QKD system (BB84, IDQuantique Clavis2) was integrated in the testbed of section 2 (Fig. 1), adding a quantum channel in an adjacent core of the MCF. QKD 1 coexist in the same core with the classical channels meanwhile the quantum channel of QKD 2 is configured without classical channels. Fig. 7 shows the QBER and BER vs launch power into the

MCF. In this case, the QBER of the QKD 1 is maintained relatively constant, with an average of 1.7%. The QKD 2 system is affected by the adjacent cores with classical signal power and a QBER change from 2.6% to 5% is observed when the launch power into the MCF is increased from -22 dBm to -9 dBm.

As observed in Fig. 7, the classical channels improve by increasing the transmitted power obtaining an average BER of 9.5×10^{-5} at a launched power of -9.5 dBm. The performance of the classical channels was measured by selecting the output of an adjacent core and receiving the signals in the BVT after demultiplexing. More importantly, the system operation is demonstrated over a dynamic range of ~10 dB of launched power into the MCF, with keys being generated from both quantum systems and simultaneous transmission of classical channels. It is important to mention in here that for longer lengths of MCFs, the effect of the Raman noise is more evident and should be considered while designing inter-datacenters architectures with interconnection distances of tens of kilometers [39]. However, it has been demonstrated that Raman noise is also evident even at short optical fiber lengths [40].
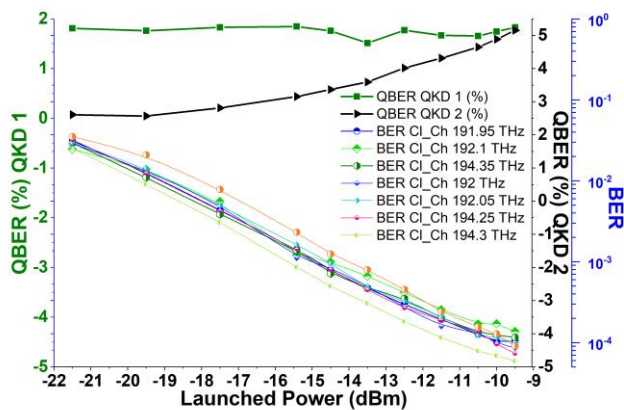

Fig. 7. Performance evaluation of the coexistence of two DV-QKD Channels and 9.8Tb/s Classical Channels over a 7-core MCF.

VI. Conclusion

The coexistence of a DV-QKD channel and 56x200 Gb/s classical channels was successfully demonstrated over a 1-km-long multicore fiber for a record-high coexistence transmission of 11.2 Tb/s. For the coexistence over the central core of the MCF, a minimum QBER of 3.7% and a maximum SKR of 920 b/s was demonstrated for the DV-QKD simultaneously with a minimum average pre-FEC BER of 1.28×10^{-2} for the classical channels. Investigations also prove that a minimum channel spacing of 17 nm is required in between quantum and classical channels and that the incremental addition of classical signals at different cores will degrade the quantum channel for a maximum QBER (SKR) of 5.3% (1400 b/s). Moreover, this work also demonstrated two quantum channels successfully operating over the same MCF maintaining simultaneous generation of keys for an optical power range of 10 dB. This work shows that DV-QKD can effectively coexist with carrier-grade equipment over MCF for maximum capacity and continuous key generation, being suitable for secure intra-data center applications.

References

[1] D. J. Richardson, J. M. Fini, and L. E. Nelson, "Space-division multiplexing in optical fibres," Nat. Photonics Vol 7, 354-362 (2013).

[2] K. Nakajima, T. Matsui, T. Sakamoto, S. Nozoe, and Y. Goto, "Progress on SDM Fiber Research in Japan," in Optical Fiber Communication Conference (OFC) 2019, OSA Technical Digest (Optical Society of America, 2019), paper M1E.1.

[3] G. M. Saridis, D. Alexandropoulos, G. Zervas and D. Simeonidou, "Survey and Evaluation of Space Division Multiplexing: From Technologies to Optical Networks," in IEEE Communications Surveys & Tutorials, vol. 17, no. 4, pp. 2136-2156.

[4] Peter J. Winzer, David T. Neilson, and Andrew R. Chraplyvy, "Fiber-optic transmission and networking: the previous 20 and the next 20 years [Invited]," Opt. Express 26, 24190-24239 (2018)

[5] T. Tsuritani, D. Soma, Y. Wakayama, Y. Miyagawa, M. Takahashi, I. Morita, K. Maeda, K. Kawasaki, T. Matsuura, M. Tsukamoto, and R. Sugizaki, "Field Test of Installed High-Density Optical Fiber Cable with Multi-Core Fibers toward Practical Deployment," in Optical Fiber Communication Conference (OFC) 2019, OSA Technical Digest (Optical Society of America, 2019), paper M3J.4.

[6] University of L'Aquila, Sumitomo Electric Industries, Ltd. and Optoscribe Ltd. Press Release, "The World's First Field Deployed Multi-Core Fiber Testbed for Optical Communications Installed in L'Aquila, Italy". (Sumitomo Electric, June 2019). https://global-sei.com/company/press/2019/06/prs043.html

[7] B. Zhu, "SDM Fibers for Data Center Applications," in Optical Fiber Communication Conference (OFC) 2019, OSA Technical Digest (Optical Society of America, 2019), paper M1F.4.

[8] Cisco Whitepaper, "Cisco Global Cloud Index: Forecast and Methodology, 2016–2021", 2018. pp. 1-46.

[9] Google Cloud Encryption Whitepaper, "Encryption in Transit in Google Cloud", November 2017. pp. 1-24.

[10] V. Mavroeidis, K. Vishi, MD. Zych, A. Jøsang, "The impact of quantum computing on present cryptography" International Journal of Advanced Computer Science and Applications (IJACSA), Vol. 9, No. 3, Mar. 2018. pp. 1-10. arXiv preprint arXiv:1804.00200.

[11] A. Aguado, V. Lopez, J. Martinez-Mateo, T. Szyrkowiec, A. Autenrieth, M. Peev, D. Lopez, and V. Martin, "Hybrid Conventional and Quantum Security for Software Defined and Virtualized Networks," J. Opt. Commun. Netw. 9, 819-825 (2017).

[12] Elboukhari M, Azizi M, Azizi A. "Improving TLS security by quantum cryptography. International Journal of Network Security & Its Applications" (IJNSA). 2010 Jul;2(3):87-100.

[13] A. Mink, S. Frankel and R. Perlner, "Quantum Key Distribution (QKD) and Commodity Security Protocols: Introduction and Integration", International Journal of Network Security & Its Applications (IJNSA), Vol 1, No 2, July 2009.

[14] Quantum Key Distribution; Use Cases. ETSI GS QKD 002. V1.1.1 (2010-06)

[15] S. Pirandola, U. L. Andersen, L. Banchi, M. Berta, D. Bunandar, R. Colbeck, D. Englund, T. Gehring, C. Lupo, C. Ottaviani, J. Pereira, M. Razavi, J. S. Shaari, M. Tomamichel, V. C. Usenko, G. Vallone, P. Villoresi, P. Wallden, "Advances in Quantum Cryptography" https://arxiv.org/abs/1906.01645. June, 2019.

[16] R. Nejabati, R. Wang, A. Bravalheri, A. Muqaddas, N. Uniyal, T. Diallo, R. Tessinari, R. S. Guimaraes, S. Moazzeni, E. Hugues-Salas, G. T. Kanellos, and D. Simeonidou, "First Demonstration of Quantum-Secured, Inter-Domain 5G Service Orchestration and On-Demand NFV Chaining over Flexi-WDM Optical Networks," in Optical Fiber Communication Conference Postdeadline Papers 2019, (Optical Society of America, 2019), paper Th4C.6.

[17] M. Peev, C. Pacher, R. Alléaume, C. Barreiro, J. Bouda, W. Boxleitner, T. Debuisschert, E. Diamanti, M. Dianati, J. F. Dynes, S. Fasel, S. Fossier, M. Fürst, J.-D. Gautier, O. Gay, N. Gisin, P. Grangier, A. Happe, Y. Hasani, M. Hentschel, H. Hübel, G. Humer, T. Länger, M. Legré, R. Lieger, J. Lodewyck, T. Lorünser, N. Lütkenhaus, A. Marhold, T. Matyus, O. Maurhart, L. Monat, S. Nauerth, J.-B. Page, A. Poppe, E. Querasser, G. Ribordy, S. Robyr, L. Salvail, A. W. Sharpe, A. J. Shields, D. Stucki, M. Suda, C. Tamas, T. Themel, R. T. Thew, Y. Thoma, A. Treiber, P. Trinkler, R. Tualle-Brouri, F. Vannel, N. Walenta, H. Weier, H. Weinfurter, I. Wimberger, Z. L. Yuan, H. Zbinden, and A. Zeilinger, "The SECOQC quantum key distribution network in Vienna," New J. Phys., vol. 11, 075001, 2009.

[18] A. Wonfor, J. F. Dynes, R. Kumar, H. Qin, W. W.-S. Tam, A. Plews, A. W. Sharpe, M. Lucamarini, Z. L. Yuan, R. V. Penty, I. H. White, and A. J. Shields, "High performance field trials of QKD over a metropolitan network," in Quantum Cryptography (Qcrypt), 2017, paper Th467.

[19] M. Sasaki, M. Fujiwara, H. Ishizuka, W. Klaus, K. Wakui, M. Takeoka, S. Miki, T. Yamashita, Z. Wang, A. Tanaka, K. Yoshino, Y. Nambu, S. Takahashi, A. Tajima, A. Tomita, T. Domeki, T. Hasegawa, Y. Sakai, H. Kobayashi, T. Asai, K. Shimizu, T. Tokura, T. Tsurumaru, M. Matsui, T. Honjo, K. Tamaki, H. Takesue, Y. Tokura, J. F. Dynes, A. R. Dixon, A. W. Sharpe, Z. L. Yuan, A. J. Shields, S. Uchikoga, M. Legré, S. Robyr, P. Trinkler, L. Monat, J.-B. Page, G. Ribordy, A. Poppe, A. Allacher, O. Maurhart, T. Länger, M. Peev, and A. Zeilinger, "Field test of quantum key distribution in the Tokyo QKD network," Opt. Express, vol. 19, no. 11, pp. 10387–10409, May 2011.

[20] N. Walenta, D. Caselunghe, S. Chuard, M. Domergue, M. Hagerman, R. Hart, D. Hayford, R. Houlmann, M. Legr´e, T. McCandlish et al., "Towards a north american qkd backbone with certifiable security," in Proc. Qcrypt, 2015.

[21] Bacco D, Vagniluca I, Da Lio B, Biagi N, Della Frera A, Calonico D, Toninelli C, Cataliotti FS, Bellini M, Oxenløwe LK, Zavatta A. Field trial of a finite-key quantum key distribution system in the Florence metropolitan area. arXiv preprint arXiv:1903.12501. 2019 Mar 29.

[22] Y. Mao, B.-X. Wang, C. Zhao, G. Wang, R. Wang, H. Wang, F. Zhou, J. Nie, Q. Chen, Y. Zhao et al., "Integrating quantum key distribution with classical communications in backbone fiber network," Optics express, vol. 26, no. 5, pp. 6010–6020, 2018.

[23] A. Aguado, V. López, D. López, M. Peev, A. Poppe, A. Pastor, J. Folgueira and V. Martín, "The Engineering of Software-Defined Quantum Key Distribution Networks," in IEEE Communications Magazine, vol. 57, no. 7, pp. 20-26, July 2019.

[24] R. S. Tessinari, A. Bravalheri, E. Hugues-Salas, R. Collins, D. Aktas, R. S. Guimaraes, O. Alia, J. Rarity, G. T. Kanellos, R. Nejabati, and D. Simeonidou, "Field Trial of Dynamic DV-QKD Networking in the SDN-Controlled Fully-Meshed Optical Metro Network of the Bristol City 5GUK Test Network" in proceedings of European Conference on Optical Communications (ECOC'19). Dublin, Ireland, September, 2019. Post-deadline paper (PDP) PD3.6.

[25] ID Quantique (IDQ) Quantum-Safe Security. https://www.idquantique.com/quantum-safe-security/overview/

[26] Toshiba QKD System. https://www.toshiba.eu/eu/Cambridge-Research-Laboratory/Quantum-Information/Quantum-Key-Distribution/Toshiba-QKD-system/

[27] E. Hugues-Salas, R. Wang, G. T. Kanellos, R. Nejabati and D. Simeonidou, "Co-existence of 9.6 Tb/s classical channels and a quantum key distribution (QKD) channel over a 7-core multicore optical fibre", In 2018 IEEE British and Irish Conference on Optics and Photonics (BICOP), 2018, pp. 1-4

[28] E. Hugues-Salas, Q. Wang, R. Wang, K. Rajkumar, G. T. Kanellos, R. Nejabati and D. Simeonidou, "Coexistence of 11.2 Tb/s Carrier-Grade Classical Channels and a DV-QKD Channel over a 7-Core Multicore Fibre", European Conference on Optical Communications (ECOC'19), Dublin, Ireland, Sep. 2018.

[29] P. D. Townsend, "Simultaneous quantum cryptographic key distribution and conventional data transmission over installed fibre using wavelength-division multiplexing," in Electronics Letters, vol. 33, no. 3, pp. 188-190, 30 Jan. 1997.

[30] B. Fröhlich, M. Lucamarini, J. F. Dynes, L. C. Comandar, W. W.-S. Tam, A. Plews, A. W. Sharpe, Z. Yuan, and A. J. Shields, "Long-distance quantum key distribution secure against coherent attacks", Optica, vol. 4, no. 1, pp. 163-167, 2017.

[31] J. F. Dynes, S. J. Kindness, S. W.-B. Tam, A. Plews, A. W. Sharpe, M. Lucamarini, B. Fröhlich, Z. L. Yuan, R. V. Penty and A. J. Shields, "Quantum key distribution over multicore fiber", Optics Express, Vol. 24, No. 8, pp. 8081-8087. 2016

[32] C. Cai, Y. Sun, Y. Zhang, P. Zhang, J. Niu, and Y. Ji, "Experimental wavelength-space division multiplexing of quantum key distribution with classical optical communication over multicore fiber," Opt. Express 27, 5125-5135 (2019)

[33] R. Lin, A. Udalcovs, O. Ozolins, X. Pang, L. Gan, L. Shen, M. Tang, S. Fu, S. Popov, C.Yang, W. Tong, D. Liu, T. Ferreira da Silva, G. B. Xavier and J. Chen, "Telecom Compatibility Validation of Quantum Key Distribution Co-existing with 112 Gbps/λ/core Data Transmission in Non-Trench and Trench-Assistant Multicore Fibers", European Conference on Optical Communications (ECOC'18), Rome, Italy, Sep. 2018.

[34] D. Bacco, B. Da Lio, D. Cozzolino, F. Da Ros, X. Guo, Y. Ding, Y. Sasaki, K. Aikawa, S. Miki, H. Terai, T. Yamashita, J. S. Neergaard-Nielsen, M. Galili, K. Rottwitt, U. Andersen, T. Morioka and L. K. Oxenlowe, "Boosting the secret key rate in a shared quantum and classical fibre communication system", Communications Physics, Vol. 2. No. 140. pp. 2399-3650.

[35] "Facebook Voyager Optical Platform" [Online]. https://cumulusnetworks.com/blog/facebook-voyager/

[36] "Acacia Transponders" [Online] https://acacia-inc.com/product/ac400-flex/

[37] "ID Quantique Clavis2 QKD platform" [Online]. Available: https://www.idquantique.com/resource-library/quantum-keydistribution/

[38] Feihong Ye, Toshio Morioka, "Interleaved core assignment for bidirectional transmission in multi-core fibers," in 39th European Conference and Exhibition on Optical Communication (ECOC), London, UK, 2013

[39] T. A. Eriksson, T. Hirano, B. J. Puttnam, G. Rademacher, R. S. Luís M. Fujiwara, R. Namiki, Y. Awaji, M. Takeoka, N. Wada and M. Sasaki, "Wavelength division multiplexing of continuous variable quantum key distribution and 18.3 Tb/s data channels", Commun Phys 2, 9 (2019).

[40] D. Zavitsanos, G. Giannoulis, A. Raptakis, C. Papapanos, F. Setaki, E. Theodoropoulou, G. Lyberopoulos, C. Kouloumentas and H. Avramopoulos, "Coexistence of Discrete-Variable QKD with WDM Classical Signals in the C-Band for Fiber Access Environments," 2019 21st International Conference on Transparent Optical Networks (ICTON), Angers, France, 2019, pp. 1-5.